# Low frequency backbone vibrations of individual conformational isomers: Tryptamine

Michael Schmitt,[a] Ke Feng, Marcel Böhm, and Karl Kleinermanns[b]
*Heinrich-Heine-Universität, Institut für Physikalische Chemie I, D-40225 Düsseldorf, Germany*

The low frequency vibrations of the ethylamino backbone of six conformers of tryptamine have been studied in the ground and excited states using dispersed fluorescence spectroscopy, rotationally resolved laser induced fluorescence, and *ab initio* calculations. Four low frequency vibrational modes of the backbone, which involve torsional and librational motions of the ethylamino group, have been identified. The three *anti* conformers show a substantially different vibrational pattern than the four conformers in which the amino group is in *gauche* position with respect to the pyrrole and the phenyl ring, respectively. © *2006 American Institute of Physics*. [DOI: 10.1063/1.2357593]

## I. INTRODUCTION

The three aromatic amino acid residues that are primarily responsible for the inherent fluorescence of proteins are tryptophan, tyrosine, and phenylalanine. In solution, tryptophan shows the highest fluorescence yield of the three chromophores. Tryptamine (see Fig. 1), which is the decarboxylation product of the amino acid tryptophan, has a very rich potential energy landscape, which is governed by torsional motions of the ethylamino backbone. Since these low frequency backbone vibrations are a probe of the molecular surrounding of the chromophore, we attempt to systemize these vibrations by means of laser induced fluorescence and dispersed emission spectroscopy.

For the nomenclature of the different tryptamine conformers, we use the scheme proposed by Carney and Zwier[1] Out of the 27 possible conformers of tryptamine ($3 \times 3 \times 3$ from rotation about $\tau_1$, $\tau_2$, and $\tau_3$ in Fig. 1) the 18 which have the ethylamino group in the aromatic plane have much higher ground state energies. The remaining nine conformers in which the ethylamino group is in *gauche* position to the phenyl (pyrrole) ring are called Gph (Gpy). Conformers in which the ethylamino group is pointing away from the indole chromophore are called anti. The orientation of the amino lone pair is given by the descriptors "up," "ph," "py," "out," and "in," depending if the lone pair points upwards, to the phenyl side, to the pyrrole side, away from the indole ring, or down to the indole ring. The two in conformers have so far not been observed experimentally and will not be treated in the present study.

Philips and Levy performed laser induced fluorescence (LIF) spectroscopy with a spectral resolution of 0.07 cm$^{-1}$ and obtained the first rotationally resolved electronic spectra of seven different conformers.[2] Later this work was extended to the triply deuterated conformers in the same group.[3] In the groups of Nguyen *et al.*[4] and Schmitt *et al.*[5] rotationally resolved spectra of tryptamine were taken at a resolution of about 0.01 cm$^{-1}$, mainly limited by the experimental Dop-

pler width and the Lorentzian width of the rovibronic transitions. Nguyen *et al.*[4] found all seven conformers that were described by Philips and Levy, while Schmitt *et al.*[5] could only determine six different conformers, although the missing one [$C(2)$ in the paper of Philips and Levy] has nearly the same intensity as the directly neighbored $C(1)$ conformer. In the meantime we were able to spot the reason for this discrepancy. By using successively larger nozzle diameters, the $C(2)$ intensity could be increased considerably. This finding shows that the relative amount of each conformer in the molecular beam in governed not only by the relative energies of the conformers but also by kinetic effects in the early phase of the expansion.[6] Using rotational coherence spectroscopy Connell *et al.* investigated five conformers of tryptamine and found two different recurrence times for the $C$ conformer, one being similar to $D$ and the other to $F$.[7] The permanent dipole moments of four tryptamine conformers were determined in a recent study by Nguyen and Pratt,[8] using the Stark effect on rotationally resolved electronic spectra. The ground states of the $A$ and $B$ conformers of tryptamine have also been studied using microwave spectroscopy.[9]

Dispersed fluorescence (DF) spectroscopy is a very useful method to observe vibrational energy levels over a wide energy range. Especially the investigation of the very low frequency region (terahertz region) is straightforward, while other spectroscopic (absorption) techniques are technologically demanding, mainly because bright stable terahertz sources are still not available commercially.

Since the $\pi^* \leftarrow \pi$ transition of tryptamine is mainly localized in the indole ring, only little Franck-Condon (FC) activity is expected from the ethylamino backbone vibrations. The low frequency vibrations of tryptamine are interesting, because they reflect the interaction between the backbone and the indole chromophore in relation to the different conformers and may be related to peptide folding in larger systems. In the present publication we will determine and assign the backbone vibrations of six tryptamine conformers in the electronic ground and excited states and compare the experimental results to *ab initio* calculations.

---
[a] Fax: 49-211-81-15195. Electronic mail: mschmitt@uni-duesseldorf.de
[b] Electronic mail: kleinermanns@uni-duesseldorf.de

## II. TECHNIQUES

### A. Experimental methods

A detailed description of the experimental apparatus for the dispersed fluorescence spectroscopy is given in Refs. 10 and 11, and for rotationally resolved LIF in Ref. 12. Both will therefore be described only briefly here. The fluorescence absorption and emission spectra are taken in a vacuum machine pumped with a 2000 L/s oil diffusion pump. A neodymium doped yttrium aluminum garnet (Nd:YAG) laser (Spectra Physics, Quanta Ray Indi) is used to pump a tunable dye laser (Lambda-Physik, FL3002). The laser light is frequency doubled and directed into the vacuum chamber, where it crosses the molecular beam at right angles. The sample is evaporated at 460 K, seeded into $2-3$ bar helium as carrier gas, and expanded through a pulsed nozzle with a 500 m orifice (General Valve). The emitted fluorescence light is collected perpendicularly to laser and molecular beam and is focused by a two-lens system on the entrance slit of a 1 m monochromator (Jobin Yvon, grating with 2400 grooves/mm blazed at 400 nm for first order). For fluorescence excitation the monochromator is used in zero order as mirror and the fluorescence is recorded by a photomultiplier tube (Thorn EMI 97890A).

For fluorescence emission, the monochromator can be used in first or second order and the fluorescence is dispersed onto a charged coupling device (CCD) detector [Flame Star I CCD-chip (TH7863, Thomson), $286 \times 384$ pixel (horizontal $\times$ vertical) with a pixel area of $23 \times 23$ $\mu m^2$]. The entrance slit was varied between 20 and 40 $\mu m$, depending on the intensity of the excited band. One dispersed fluorescence spectrum is obtained by summing the signal of 200 laser pulses and subtracting the background that emerges from scattered light. Fifty of these single spectra are summed up for a better signal/noise ratio. Using the grating in first order allows imaging a DF spectrum of about 500 $cm^{-1}$ simultaneously.

The experimental setup for rotationally resolved LIF consists of a ring dye laser (Coherent 899-21) operated with rhodamine 110, pumped with 6.5 W of the 514 nm line of an $Ar^+$-ion laser. Its output is coupled into an external folded ring cavity (Spectra Physics) for second harmonic generation (SHG). The molecular beam is formed by coexpanding tryptamine, heated to 190 °C and argon ($250-500$ mbars)
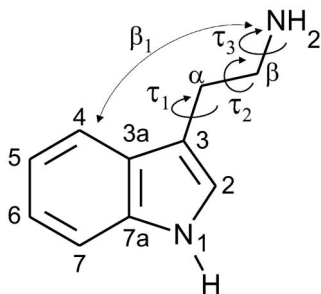
through a 100 $\mu m$ nozzle into the vacuum. The molecular beam machine consists of three differentially pumped vacuum chambers that are connected by two skimmers of 1 and 3 mm in order to reduce the Doppler width. The molecular beam is crossed at right angles in the third chamber with the laser beam 360 mm downstream of the nozzle and the resulting fluorescence is collected perpendicular to laser and molecular beam by an imaging optics. The Doppler width in this setup is 25 MHz [full width at half maximum (FWHM)]. A photomultiplier tube detects the integrated molecular fluorescence and its output is discriminated and digitized by a photon counter and transmitted to a PC for data recording and processing. Relative frequencies are determined with a quasiconfocal Fabry-Pérot interferometer with a free spectral range (FSR) of approximately 150 MHz. The absolute frequency was obtained from a recording of the iodine absorption spectrum and comparing it to the tabulated lines.[13]

### B. Theoretical methods

In this work, the structures of the seven experimentally observed conformers of tryptamine in the electronic ground state have been optimized at the Møller-Plesset second order perturbation theory MP2/6-311G$(d,p)$ level with the GAUSSIAN 98 program package.[14] The self-consistent-field (SCF) convergence criterion used throughout the calculations is an energy change below $10^{-8}$ hartree, while the convergence criteria for the gradient optimization of the molecular geometry were $\delta E/\delta r < 1.5 \times 10^{-5}$ hartree/bohr and $\delta E/\delta \phi < 1.5 \times 10^{-5}$ hartree/deg, respectively. The vibrational frequencies have been calculated using the analytical gradients.

The equilibrium geometry and vibrational frequencies of the electronic ground state of tryptamine were also determined using the B3-LYP functional[15,16] employing the valence triple zeta basis set with polarization functions $(d,p)$ from the TURBOMOLE library.[17,18] The geometry of the $L_b$ electronically excited singlet states was fully optimized by means of a time dependent density functional theory (TD-DFT) gradient using the B3-LYP functional.[19] The vibrational frequencies have been calculated using the analytical second derivatives for the ground state and the numerical second derivatives for the electronically excited state. All DFT and TDDFT calculations were carried out utilizing the TURBOMOLE package, version 5.6.[20]

## III. RESULTS

### A. Theoretical results

The calculated vibrational frequencies in the ground and electronically excited states of the Gpy(out) conformer, obtained from MP2/6-311G$(d,p)$ and TDDFT/TZVP calculations, are summarized in Table I.

The nomenclature is adopted from Varsanyi[21] for ortho-di-light-substituted benzene derivatives and is completed for vibrations of the five-membered ring following the scheme given in Ref. 11 and for the backbone vibrations of the ethylamino group. Many of the chromophore modes couple only weakly to the backbone vibrations and retain the original displacement vectors of ortho-di-light-substituted benzene derivatives and can therefore be classified according to the



FIG. 1. Atomic numbering of tryptamine and definitions of the four low frequency vibrations of the backbone. $\tau_1$, $\tau_2$, and $\tau_3$ are three torsional vibrations around the $C_1-C_\alpha$, $C_\alpha-C_\beta$, and $C_\beta-N$ single bonds, respectively. $\beta_1$ is the bending vibration between the backbone and the indol ring.

TABLE I. Electronic ground state vibrations, calculated at the MP2/6-311G$(d,p)$ level of theory, and excited state vibrations calculated at the TDB3-LYP/TZVP level along with the assignments of the vibrational modes of the $A$ conformer of tryptamine. All frequencies are given in cm$^{-1}$. Modes marked with $^\dagger$ are localized mainly in the ethylamino backbone, modes marked with $^*$ mainly in the pyrrole moiety.

| No. | Mode | $S_0$ MP2 | $S_1$ TDDFT | No. | Mode | $S_0$ MP2 | $S_1$ TDDFT |
|---|---|---|---|---|---|---|---|
| 1 | $\tau_1^\dagger$ | 41 | 42 | 34 | 18a | 1154 | 1108 |
| 2 | $\beta_1^\dagger$ | 77 | 79 | 35 | 9a | 1173 | 1172 |
| 3 | $\tau_2^\dagger$ | 131 | 121 | 36 | NH$_2$ twist$^\dagger$ | 1183 | 1165 |
| 4 | 10b | 171 | 164 | 37 | CH$_2$ twist$^\dagger$ | 1228 | 1201 |
| 5 | 10a | 210 | 159 | 38 | 13 | 1265 | 1259 |
| 6 | $N_{inv}/\tau_1/\tau_3^\dagger$ | 229 | 229 | 39 | 3/ | 1275 | 1234 |
| 7 | $\gamma$NH/$\tau_3^\dagger$ | 258 | 241 | 40 | 18b/CH,NH | 1331 | 1291 |
| 8 | $N_{inv}/\tau_1/\tau_3^\dagger$ | 300 | 279 | 41 | C$_\beta$H$_2$ twist$^\dagger$ | 1354 | 1337 |
| 9 | $N_{inv}/\tau_1/\tau_2^\dagger$ | 359 | 344 | 42 | C$_\alpha$H$_2$ bend$^\dagger$ | 1376 | 1366 |
| 10 | 16b | 391 | 307 | 43 | 3/$\nu$CC$^*$ | 1387 | 1433 |
| 11 | 4 | 408 | 379 | 44 | C$_\beta$H$_2$ wag$^\dagger$ | 1435 | 1413 |
| 12 | 9b | 456 | 458 | 45 | 14/$\delta$CH,NH$^*$ | 1449 | 1409 |
| 13 | CCN bend$^\dagger$ | 469 | 462 | 46 | 19b/$\delta$NH | 1470 | |
| 14 | 6a | 533 | 510 | 47 | C$_\alpha$H$_2$ bend$^\dagger$ | 1487 | 1483 |
| 15 | 6b | 562 | 572 | 48 | 19a | 1517 | 1447 |
| 16 | $\gamma$NH$^*$ | 588 | 524 | 49 | C$_\beta$H$_2$ bend$^\dagger$ | 1531 | 1504 |
| 17 | 16a | 620 | 660 | 50 | 19a/C$_\beta$H$_2$ bend | 1534 | 1514 |
| 18 | CCC bend$^\dagger$ | 707 | 571 | 51 | $\nu$CC$^*$ | 1601 | 1780 |
| 19 | 11 | 715 | 577 | 52 | 8a | 1619 | 1473 |
| 20 | $\gamma$CH$^*$ | 747 | 615 | 53 | NH$_2$ bend$^\dagger$ | 1641 | 1653 |
| 21 | 1 | 770 | 745 | 54 | 8b | 1676 | 1586 |
| 22 | 17a | 801 | 606 | 55 | $\nu_s$C$_\beta$H$^\dagger$ | 3017 | 2956 |
| 23 | 17b | 859 | 691 | 56 | $\nu_s$C$_\alpha$H$^\dagger$ | 3069 | 3022 |
| 24 | C$_\alpha$H$_2$ twist$^\dagger$ | 878 | 838 | 57 | $\nu_{as}$C$_\beta$H$^\dagger$ | 3109 | 3051 |
| 25 | 5 | 880 | 757 | 58 | $\nu_{as}$C$_\alpha$H$^\dagger$ | 3132 | 3072 |
| 26 | 12 | 891 | 865 | 59 | $\nu_{as}$CH | 3196 | 3185 |
| 27 | NH$_2$ wag$^\dagger$ | 910 | 878 | 60 | $\nu_s$CH | 3202 | 3192 |
| 28 | C$_\alpha$H$_2$ wag$^\dagger$ | 939 | 901 | 61 | $\nu_{as}$CH | 3214 | 3204 |
| 20 | 18b | 1030 | 950 | 62 | $\nu_s$CH | 3226 | 3211 |
| 30 | CH$_2$ twist$^\dagger$ | 1037 | 1010 | 63 | $\nu_{py}$CH$^*$ | 3272 | 3265 |
| 31 | CH$_2$ twist$^\dagger$ | 1103 | 1095 | 64 | $\nu_s$NH$_2$ | 3524 | 3485 |
| 32 | $\delta$CH,NH$^*$ | 1116 | 1077 | 65 | $\nu_{as}$NH$_2^*$ | 3618 | 3566 |
| 33 | C$_\alpha$H$_2$ wag$^\dagger$ | 1131 | | 66 | $\nu_{py}$NH | 3696 | 3661 |

Varsanyi scheme. Nevertheless, in an unsymmetrical molecule of this size the unequivocal description of modes poses a problem, and the vibrational motions should preferably be viewed with a graphical visualization program, to inspect and assign the vibrations. MOLDEN frequency files (.molf) and GAUSSIAN.log files containing geometries and vibrational modes of all tryptamine conformers investigated in this study can be obtained from one of the authors' homepage.[23]

TABLE II. Electronic ground state low frequency vibrations calculated at the MP2/6-311$(d,p)$ (B3-LYP/TZVP) level and assignment of the vibrational modes of the seven tryptamine conformers. All frequencies are given in cm$^{-1}$. For a description of the modes, see text.

| Mode | $A$ Gpy(out) | $B$ Gpy(up) | $C(1)$ Gph (out) | $F$ Gph(up) | $D$ anti(py) | $E$ anti(up) | $C(2)$ anti(ph) |
|---|---|---|---|---|---|---|---|
| $\tau_1$ | 41(45) | 40(37) | 71(50) | 55(42) | 58(61) | 56(45) | 58(62) |
| $\beta_1$ | 77(83) | 80(78) | 93(87) | 83(80) | 78(81) | 78(80) | 80(82) |
| $\tau_2$ | 131(136) | 129(129) | 135(124) | 132(129) | 87(91) | 91(86) | 89(95) |
| 10b | 171(178) | 170(176) | 198(203) | 188(196) | 180(197) | 181(196) | 180(197) |
| 10a | 210(219) | 211(219) | 207(215) | 206(216) | 210(220) | 211(219) | 210(220) |
| $N_{inv}/\tau_1/\tau_3$ | 229(266) | 236(286) | 223(230) | 229(232) | 232(236) | 232(237) | 227(226) |
| $\gamma$NH/$\tau_3$ | 258(240) | 330(243) | 314(331) | 341(301) | 246(241) | 304(290) | 247(324) |
| $N_{inv}/\tau_1/\tau_2/\tau_3$ | 300(332) | 271(327) | 281(273) | 284(231) | 277(326) | 275(322) | 275(252) |
| $N_{inv}/\tau_1/\tau_2$ | 359(385) | 354(377) | 365(384) | 355(329) | 345(346) | 334(338) | 349(347) |
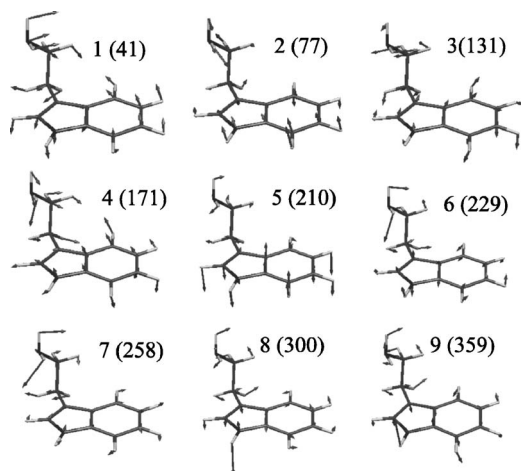
FIG. 2. Vibrational modes of the Gpy(out) conformer of tryptamine below 360 cm$^{-1}$. Numbering of the modes refers to Table I.



FIG. 3. Fluorescence excitation spectrum in the region of the electronic origins of the conformers $A$ to $F$ of tryptamine. Bands marked with an asterisk are excited to obtain the dispersed florescence spectra. Bands marked with a dagger have been measured with rovibronic resolution (see Sec. III C).

Table II compares the low frequency vibrational modes below 360 cm$^{-1}$ (shown in Fig. 2) of the seven conformational isomers of tryptamine in this study.

Mode 1 ($\tau_1$) can be described by the torsional motion about the C$_3$–C$_\alpha$ single bond, mode 3 ($\tau_2$) as torsion about the C$_\alpha$–C$_\beta$ bond, and mode 7 ($\gamma$NH/$\tau_3$) as torsion around the C$_\beta$–N$_{10}$ bond, but with admixture of a NH out-of-plane vibration. Mode 2 ($\beta_1$) has mostly character of a bending motion of the backbone relative to the indole ring. Mode 4 (10b) is the twisting mode of the indole chromophore and mode 5 (10a) is the butterfly mode. Mode 6 ($N_{\text{inv}}/\tau_1/\tau_3$) is mainly composed of a ring twisting motion, with a strong pyrrolic NH inversion, $\tau_1$, and $\tau_3$ admixtures. Mode 8 can best be described as coupled NH inversion with $\tau_1$, $\tau_2$, and $\tau_3$ vibrations. Mode 9 consists of the pyrrolic N inversion with additional $\tau_1$ and $\tau_2$ admixture. Especially mode $\tau_3$ couples strongly to the NH out-of-plane vibrations or to the pyrrolic N inversion, so that an unequivocal description in terms of pure torsional motions can hardly be given. Pyrrolic N inversion and NH out of plane modes are similar, but in the former one, the adjacent atoms to the central nitrogen move out of phase with respect to the N, while in the latter, the nitrogen stays in the indole plane and only the adjacent H atom moves out of the plane.

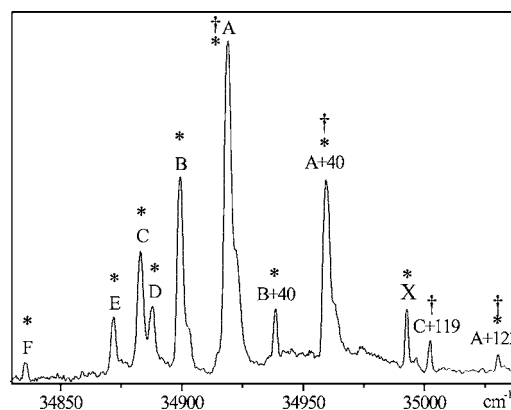The excited state low frequencies of all seven conform-ers have been calculated using the numerical second derivatives at the TDDFT optimized structure obtained with the B3-LYP functional and the TZVP basis set from the TURBO-MOLE library[20] and are given in Table III. The torsional vibrations $\tau_1$, $\tau_2$, and $\tau_3$ and the wagging vibration of the backbone $\beta_1$ have similar frequencies as in the electronic ground state, since the geometry of the ethylamino backbone is not altered upon electronic excitation to the $^1L_b$ state.[22] On the other hand, modes 4–6, 8, and 9, which are localized mainly in the aromatic ring, show larger shifts relative to the ground state frequencies.

## B. Laser induced fluorescence spectra of tryptamine

The fluorescence excitation spectrum of tryptamine in the range of the low frequency vibrations is shown in Fig. 3. The electronic origins of the $E$ (34 868 cm$^{-1}$) and $F$ (34 832 cm$^{-1}$) conformers are considerably weaker than the $A$ (34 916 cm$^{-1}$) and $B$ (34 896 cm$^{-1}$) conformers.

The electronic origins of the $C(1)$ (34 879 cm$^{-1}$), $C(2)$ (34 880 cm$^{-1}$), and $D$ (34 884 cm$^{-1}$) conformers are spectrally very close and of intermediate intensity. Nguyen *et al.*[4] and Schmitt *et al.*[5] independently related band $A$ to the Gpy-(out) conformer, band $B$ to Gpy(up), band $C(1)$ to Gph(out), band $E$ to anti(up), and band $F$ to Gph(up). A different as-

TABLE III. Low frequency vibrations of the electronically excited $^1L_b$ state calculated at the TD-B3-LYP/TZVP level and assignment of the vibrational modes of the seven tryptamine conformers. All frequencies are given in cm$^{-1}$.

| Mode | $A$ Gpy(out) | $B$ Gpy(up) | $C(1)$ Gph (out) | $F$ Gph(up) | $D$ anti(py) | $E$ anti(up) | $C(2)$ anti(ph) |
|---|---|---|---|---|---|---|---|
| $\tau_1$ | 42 | 47 | 57 | 53 | 56 | 55 | 57 |
| $\beta_1$ | 79 | 76 | 83 | 77 | 79 | 77 | 80 |
| $\tau_2$ | 121 | 122 | 122 | 125 | 99 | 96 | 103 |
| 10b | 164 | 159 | 176 | 175 | 167 | 167 | 166 |
| 10a | 156 | 163 | 160 | 162 | 158 | 159 | 159 |
| $N_{\text{inv}}/\tau_1/\tau_3$ | 229 | 228 | 222 | 226 | 232 | 237 | 224 |
| $\gamma$NH/$\tau_3$ | 241 | 261 | 249 | 264 | 240 | 295 | 246 |
| $N_{\text{inv}}/\tau_1/\tau_2/\tau_3$ | 279 | 305 | 277 | 306 | 264 | 257 | 261 |

signment has been made for the anti(ph) and anti(py) conformers. Nguyen *et al.* assigned the tryptamine *D* band to the anti(ph) conformer based on a comparison of the differences of rotational constants of pairs of conformers to the results of *ab initio* calculations. Schmitt *et al.* made an assignment of the *D* band to the anti(py) conformer, on the basis of the rotational constants of the triply deuterated conformers. At the resolution of the current LIF spectra, the close-lying $C(1)$ and $C(2)$ origins cannot be resolved.

The band at $+41$ cm$^{-1}$ ($+40$ cm$^{-1}$) above the electronic origin of the *A* (*B*) conformer in the fluorescence excitation spectrum can be assigned to the torsional vibration $\tau_1$ of the respective conformer in the electronically excited state. The band at $+74$ cm$^{-1}$ above the origin of the *A* conformer (marked with "X" in Fig. 3) does not belong to the tryptamine spectra and might be a decomposition product. 83 cm$^{-1}$ above the *A* origin a band is observed that can be assigned to a vibronic band of the *C* conformer (marked with "$C+119$" in Fig. 3) on the basis of rotationally resolved LIF spectroscopy (see Sec. III C). A weak band at $+123$ cm$^{-1}$ above the *A* origin is assigned to the $\tau_2$ mode. The alternative assignment to the second overtone of the $\tau_1$ vibrations can be excluded on the basis of the emission spectrum obtained by exciting through this band (*vide infra*).

## C. Rotationally resolved spectra of the vibronic bands

Alternatively to hole burning schemes, rotationally resolved electronic spectra can be used to distinguish between vibronic bands belonging to different conformers, since the ground state rotational constants, extracted from the fit of the rovibronic band, will be those of the electronic origin, while the excited state constants contain both the geometry changes caused by the electronic excitation and an additional part due to the squared atomic displacements along the respective normal mode in the electronically excited state. Figure 4 shows the rotationally resolved spectra of the electronic origin of the *A* conformer, of the $0,0(A)+41$ cm$^{-1}$, and of the $0,0(A)+123$ cm$^{-1}$ bands. Table IV compares the changes of the rotational constants upon electronic excitation between the different vibronic bands. No rotationally resolved LIF spectrum could be obtained at the position marked with X (formally $A+74$ cm$^{-1}$) in Fig. 3, which makes it likely that this band is due to thermal decomposition of the tryptamine sample. The evaluation of the rotationally resolved spectrum of the band marked with $0,0(C)+119$ yields the ground state rotational constants of the $C(1)$ conformer, so that this band can safely be assigned to the $0,0(C)+119$ cm$^{-1}$ vibronic band.

The excited state *A* rotational constants of the vibronic bands are in general larger than those of the zero-point level (ZPL), while the *B* and *C* constants are generally smaller. The excited state *A* rotational constant of the $0,0(A)+41$ cm$^{-1}$ band increases by 6.86 MHz compared to the ZPL (given by $\Delta\Delta A$ in Table IV), a value which is considerably larger than the change of the $0,0(A)+123$ cm$^{-1}$ band (1.06 MHz).
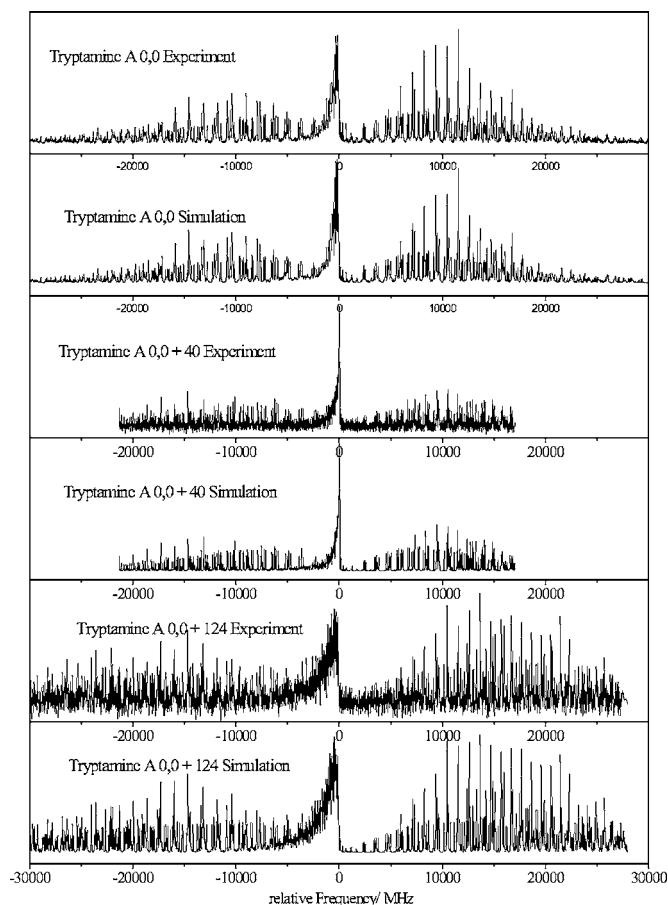
A simple model calculation shows that indeed the



FIG. 4. Rotationally resolved fluorescence excitation spectrum of the electronic origin, the $0,0+41$ cm$^{-1}$, and the $0,0+124$ cm$^{-1}$ bands of the tryptamine *A* conformer.

$0,0(A)+41$ cm$^{-1}$ band is due to the $\tau_1$ vibration. The changes of the moments of inertia upon vibronic excitation have been calculated from the scaled squared displacement vectors for this torsional motion at TDB3-LYP/VTZP level of theory. With the scaling factor chosen, so that a $\Delta\Delta A$ of 7 MHz is reproduced, the $\Delta\Delta B$ and $\Delta\Delta C$ values are $-2$ and $-1$ MHz, respectively, close to the experimentally determined changes (see Table IV). For the vibration at 123 cm$^{-1}$ the scaled rotation-vibration corrections using the $\tau_2$ displacements amount to 1, 0.6, and 0.5 MHz, again close to the $\Delta\Delta B_g$ values from Table IV. The simple model predicts all changes for this mode to be slightly positive, while experiment shows $\Delta\Delta B$ and $\Delta\Delta C$ to be small and negative. This discrepancy is mainly caused by the oversimplification of taking only harmonic, one-dimensional contributions into account. Nevertheless, vibrational assignments are possible, comparing the *ab initio* predicted vibronic contributions to the ZPL rotational constants with the experimental ones. Mode $0,0(C)+119$ cm$^{-1}$ has very similar vibronic contributions as $0,0(A)+123$ cm$^{-1}$ and can therefore be assigned to the same mode $\tau_2$ of the Gph(out) conformer.

## D. Fluorescence emission spectra

### 1. Emission spectra through the electronic origins

The low frequencies in the fluorescence emission spectra, obtained via excitation of the electronic origins of the different conformers, are assigned to the respective vibra-

TABLE IV. Molecular parameters of the low frequency bands in the region of the electronic origins of the tryptamine conformers. The $\Delta B_g$ are defined as $B'_g - B''_g$, $g = A, B, C$. The $\Delta\Delta B_g$ are defined as $\Delta B_g[0,0(A)+X] - \Delta B_g[0,0(A)]$ and $\Delta B_g[0,0(C)+X] - \Delta B_g[0,0(C)]$, respectively.

| | 0,0(A) | 0,0(A)+41 | 0,0(A)+123 | 0,0(C) | 0,(C)+119 |
|---|---|---|---|---|---|
| $A''$ (MHz) | 1731.02 | 1731.02 | 1731.02 | 1594.16 | 1593.62 |
| $B''$ (MHz) | 682.04 | 682.04 | 682.04 | 755.84 | 755.37 |
| $C''$ (MHz) | 551.56 | 551.56 | 551.56 | 561.39 | 561.04 |
| $\nu_0$ (cm$^{-1}$) | 34915.64 | 34956.77 | 35038.41 | 34879.22 | 34998.57 |
| $\phi$ (deg) | 72 | 84 | 80 | 77 | 77 |
| $\theta$ (deg) | 14 | 2 | 2 | 18 | 11 |
| $\Delta A$ (MHz) | −7.00 | −0.14 | −5.94 | −6.78 | −5.32 |
| $\Delta B$ (MHz) | −9.36 | −10.79 | −10.14 | −12.76 | −14.34 |
| $\Delta C$ (MHz) | −6.98 | −8.10 | −7.53 | −7.19 | −7.79 |
| $\Delta\Delta A$ (MHz) | 0 | 6.86 | 1.06 | 0 | 1.46 |
| $\Delta\Delta B$ (MHz) | 0 | −1.43 | −0.78 | 0 | −1.58 |
| $\Delta\Delta C$ (MHz) | 0 | −1.12 | −0.55 | 0 | −0.60 |

tional modes using the results of the *ab initio* calculations described in Sec. III A.

We start with the assignments of the two Gpy conformers. The first trace of Fig. 5 shows the fluorescence emission spectrum, obtained via excitation of the vibrationless origin of the A conformer. Table II compiles the vibrational frequencies and assignments of all conformers. We observe the lowest frequency mode $\tau_1$ (torsion about the $C_3$-$C_\alpha$ single bond) of the A conformer (see trace A) at 43 cm$^{-1}$ and of the B conformer (see trace B in Fig. 5) at 41 cm$^{-1}$. The corresponding MP2/6-311G$(d,p)$ calculated frequency of this mode of the Gpy(out) conformer is 41 cm$^{-1}$ and of the Gpy(up) conformer 40 cm$^{-1}$ (see Table II). The first overtone of this vibration is observed at 86 cm$^{-1}$ for the A conformer. In the B conformer this band coincides with the energetically following vibration $\beta_1$, which is calculated at 80 cm$^{-1}$ for the B and at 77 cm$^{-1}$ for the A conformer. In the spectrum of the A conformer this band is observed at 81 cm$^{-1}$. A weak band at 124 cm$^{-1}$ in the spectrum of the A conformer is assigned to the second overtone of the $\tau_1$ vibration. For a confirmation of this assignment of the $3\tau_1$ band, see Sec. III D 2. The band at 133 (128) cm$^{-1}$ in the spectrum of the A(B) conformer is

assigned to the torsion around the $C_\alpha$-$C_\beta$ single bond ($\tau_2$). The following two bands at 177 and 215 cm$^{-1}$ are the fundamentals of two ring deformations, namely, the 10b (ring twist) and 10a (ring butterfly), respectively. The torsion about the $C_\beta$-$N_{10}$ ($\tau_3$) bond strongly mixes with the other torsional motions and with NH out-of-plane motions in the pyrrole ring. The mode closest to a $\tau_3$ torsion (see Fig. 2) is calculated at 258 cm$^{-1}$ and can be assigned to the experimentally observed transition at 256 cm$^{-1}$ in the spectrum of the A conformers. The respective transition for the B conformer is observed at a substantially higher frequency of 330 cm$^{-1}$, also in close agreement with the calculations. All other observed transitions are combination bands or overtones of the described modes and can be found in Table V.

In the following we will give the assignments of the vibrational bands of the two Gph conformers [C(1) and F] (see traces C and F in Fig. 5). The lowest frequency $\tau_1$ band can only be observed in the spectrum of the C(1) conformer at 60 cm$^{-1}$. It is calculated at 71 cm$^{-1}$, considerably higher than the respective vibration in the Gpy conformers (see Table II). The mode $\beta_1$ is observed for conformer C(1) at 87 cm$^{-1}$ and for F at 77 cm$^{-1}$, in good agreement with the theoretical values of 93 and 80 cm$^{-1}$, respectively. They are close to the respective values of the Gpy conformers. The band at 128 cm$^{-1}$ of both conformers is assigned to the $\tau_2$ vibration. Also this vibration has nearly the same frequency in the Gpy and Gph conformers. The ring butterfly mode (10a) is observed at 201 cm$^{-1}$, and the $\gamma$NH/$\tau_3$ band at 331 cm$^{-1}$ for the C(1) conformer. Both vibrations are too weak to be detected in the emission spectrum of the F conformer.

In the following we will discuss the vibrations of the anti conformers. Two of the anti conformers (ph and py) have been assigned differently in Refs. 1, 4, and 5. Let us start with the anti(up) conformer, which is indisputably assigned to the E conformer by all groups and whose DF spectrum is shown in trace E of Fig. 5. The lowest frequency mode $\tau_1$ in the DF spectra of E is observed at 55 cm$^{-1}$. The $\beta_1$ mode of anti(up) is observed at 78 cm$^{-1}$, in perfect agreement with the MP2 calculations given in Table II. While in the spectra of the Gpy and Gph conformers mode $\tau_2$ is observed con-
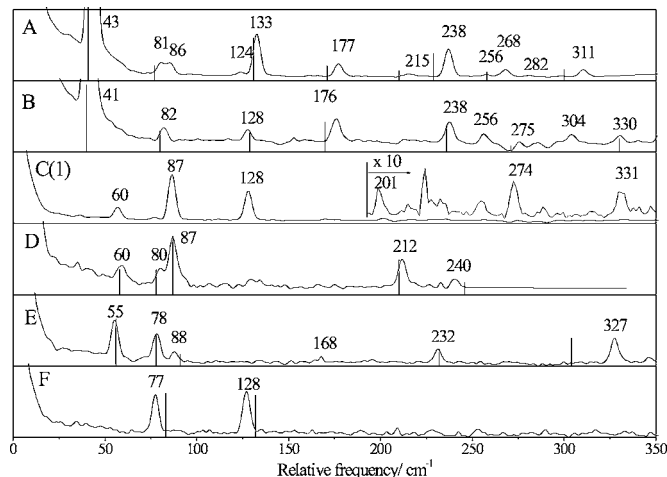


FIG. 5. Fluorescence emission spectra obtained via excitation of the electronic origins of the conformers A to F. The vertical lines represent the MP2 calculated frequencies.

TABLE V. Experimental ground state ($S_0$) intermolecular vibrational frequencies observed after excitation of all $S_1$ states and assignments of the motions. All frequencies are given in cm$^{-1}$.

| Assignment | $A$ Gpy(out) | $B$ Gpy(up) | $C(1)$ Gph(out) | $D$ anti(py) | $E$ anti(up) | $F$ Gph(up) |
|---|---|---|---|---|---|---|
| $\tau_1$ | 43 | 41 | 60 | 60 | 55 | |
| $\beta_1$ | 81 | 82 | 87 | 80 | 78 | 77 |
| $2\tau_1$ | 86 | | | | | |
| $\tau_2$ | 133 | 128 | 128 | 87 | 88 | 128 |
| $3\tau_1$ | 124 | | | | | |
| $\beta_1+\tau_2$ | | | | | 168 | |
| 10b | 177 | 176 | | | | |
| 10a | 215 | | 201 | 212 | | |
| $N_{\mathrm{inv}}/\tau_1/\tau_3$ | 238 | 238 | | | 232 | |
| $\gamma$NH$/\tau_3$ | 256 | 330 | 331 | 240 | 327 | |
| 10b$+\beta_1$ | | 256 | | | | |
| $N_{\mathrm{inv}}/\tau_1/\tau_2/\tau_3$ | 268 | 275 | 274 | | | |
| $\tau_2+10b$ | 311 | 304 | | | | |

stantly around 130 cm$^{-1}$, this band shifts down to 88 cm$^{-1}$ in the spectrum of the anti(up) conformer. The mode $\gamma$NH$/\tau_3$ is assigned to the transition at 327 cm$^{-1}$. According to the results of rotationally resolved LIF spectroscopy in the groups of Nguyen *et al.* and Schmitt *et al.* the $C(2)$ band and the $D$ band have to be assigned to the conformers anti(py) and anti(ph),[4] or vice versa.[5] In the emission spectrum of the $D$ band the $\tau_1$ vibration is found at 60 cm$^{-1}$, close to the theoretical value of 58 cm$^{-1}$ for both the anti(py) and anti(ph) conformers from Table II. The second torsional mode is shifted down to 78 cm$^{-1}$ for anti(py), like in the spectrum of the anti(up) conformer, and down to 80 cm$^{-1}$ for anti(ph). Therefore, this mode serves as good indicator whether the observed conformer is Gpy/Gph on one hand side or one of the anti conformers. The $\gamma$NH$/\tau_3$ band of the $D$ band is found experimentally at 240 cm$^{-1}$, which is the lowest value of this vibrational frequency for all conformers, in good agreement with calculated frequencies of 246 cm$^{-1}$ for anti(py) and 247 cm$^{-1}$ for anti(ph). The largest calculated difference of vibrational frequencies for the modes of anti(py) and anti(ph) is 6 cm$^{-1}$. Therefore, no distinction between the different assignments for the bands can be made on the basis of the DF spectra. We also tried to obtain dispersed fluorescence spectra upon excitation of the $C(2)$ band, but no difference in the emission spectra could be obtained upon shifting the excitation wavelength from the maximum of the $C$ band successively to the blue. The strongest bands, which can be expected for the $C(2)$ band independent of the assignment of this band to anti(py) or anti(ph), should be the $\tau_1$ and the $\tau_2$ vibrations. Unfortunately, $\tau_1$ coincides with the same vibration of $C(1)$, while the predicted value of 87 cm$^{-1}$ for the $\tau_2$ vibration coincides with that of the $\beta_1$ vibration of $C(1)$. Thus, only slightly changed intensities of the $C(1)$ and $C(2)$ bands can be expected, which are not sufficient for a distinction of the two conformers.

### 2. Emission spectra through excited vibronic bands

Figure 6 shows the DF spectra, which are obtained via excitation of the vibronic bands at 40, 124, and 228 cm$^{-1}$ of the Gpy(out) conformer. The propensity rule immediately allows the assignment of the vibration $\tau_1$ to the excited state band at 40 cm$^{-1}$, of the vibration $\tau_2$ to the excited state band at 124 cm$^{-1}$, and of the vibration $N_{\mathrm{inv}}/\tau_1/\tau_3$ to the excited state band at 228 cm$^{-1}$.

The vibrational progression observed in the emission spectrum through the $\tau_1$ mode includes the (resonant) $^1_0\tau_1$, the $^1_1\tau_1$ at 43 cm$^{-1}$, and the $^1_2\tau_1$ transition at 86 cm$^{-1}$. Obviously, there is a strong anharmonic coupling between the $\tau_1$ and the $\tau_2$ mode, as can be inferred from the emission spectrum via the excited $\tau_2$ mode. The strongest band in emission is the $^1_1\tau_2$ mode at 133 cm$^{-1}$, but additionally a long Franck-Condon progression in the $\tau_1$ mode is observed, which continues until the $^1_3\tau_1$ transition at 124 cm$^{-1}$. The spectrum in trace $b$ of Fig. 6 also shows that the band at 177 cm$^{-1}$ has to be attributed to a fundamental and not to a combination band of the 133 cm$^{-1}$ band with one quantum of the $\tau_1$ mode, since the fundamental of the $\tau_1$ vibration is very weak in this spectrum, and only the first overtone at 87 cm$^{-1}$ shows up with higher intensity.
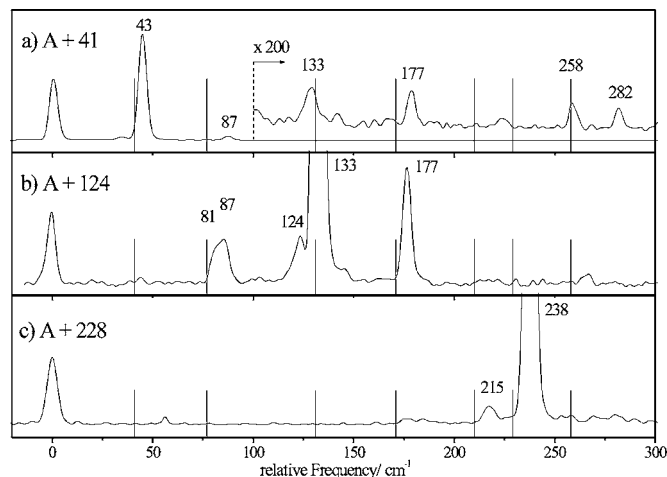


FIG. 6. Fluorescence emission spectra obtained via excitation of the vibronic bands $0,0+41$, $0,0+124$, and $0,0+228$ of conformer $A$. The vertical lines represent the MP2 calculated frequencies

TABLE VI. Schematic summary of the 24 vibrations of the ethylamino backbone of tryptamine.

| No. | Vibrational mode | range (cm$^{-1}$) |
|---|---|---|
| 4 | Back bone vibrations | 30–350 |
| 3 | C/N–C stretching | 700–1200 |
| 2 | CCC/CCN bending | 700–1200 |
| 3 | $CH_2/NH_2$ twist | 900–1500 |
| 3 | $CH_2/NH_2$ wagging | 900–1500 |
| 3 | $CH_2/NH_2$ bending | 1400–1700 |
| 6 | C/N–H stretching | 3000–3500 |

## IV. DISCUSSION

### A. Systematics of the vibrations on the ethylamine backbone

A nonlinear molecule containing $N$ atoms has $3N-6$ fundamental or normal modes of vibration. The ethylamine backbone of tryptamine with ten mass points (nine atoms and the indole ring) would have 24 different normal modes of vibration. The vibrations in Table VI are arranged with the 24 motions in ascending frequency. Four ground state low-vibrational motions of the tryptamine conformers can be grouped, which include bending between the indole ring and the $NH_2$ group and three rotations of the alkylamino side chain: two around the C–C single bonds and one around the C–N bond. The C/N–C bond stretching and bending vibrations appear in the range between 700 and 1200 cm$^{-1}$. Twisting and wagging motions of the $CH_2$ and $NH_2$ groups are observed between 900 and 1500 cm$^{-1}$, while the respective bending motions are located at higher frequencies between 1400 and 1700 cm$^{-1}$. The C/N–H stretching vibrations appear at the highest frequencies between 3000 and 3500 cm$^{-1}$.

For the low frequency backbone vibrations, the amino group position (anti or *gauche*) with respect to the indole chromophore plays a major role. The frequency differences of the four backbone modes between the different conformers can be qualitatively explained by the changes in the force constants of the respective vibration. According to the observation, all anti conformers have lower vibrational frequencies in the mode $\tau_2$, which can be traced back to different force constants for this torsional motion.

The harmonic force constants of the mode $\tau_2$ of anti(py), anti(ph), and anti(up) on the basis of *ab initio* calculations at the MP2/6-311G$(d,p)$ level are 0.0100, 0.0090, and 0.0084 mdyn/Å, respectively. The force constants of Gpy(out), Gpy(up), Gph(out), and Gph(up) are 0.0247, 0.0213, 0.0302, and 0.0242 mdyn/Å, respectively, about three times as large as the force constants of the anti conformers. Consequently, the mode $\tau_2$ of the anti conformers is observed at lower frequencies around 90 cm$^{-1}$, while for the *gauche* conformers vibrational frequencies around 130 cm$^{-1}$ are observed. This reason for this effect is the interaction of the amino group of the backbone with the indole ring in the case of the *gauche* conformers, causing the $\tau_2$ potential to be stiffer.

On the other hand, the $\tau_1$ force constants of the Gpy conformers are small (0.004 mdyn/Å for both), and considerably larger for all three anti conformers (0.007 mdyn/Å),

while they are quite different for the two Gph conformers [ 0.011 mdyn/Å for Gph(out) and 0.06 mdyn/Å for Gph(up)], reflecting the ranges of the $\tau_1$ frequencies in the different conformers. Compared to the large differences of the force constants, the reduced masses of the different conformers are quite similar and are thus not responsible for the experimentally observed differences.

## V. CONCLUSIONS

We have assigned the low frequency backbone vibrations of tryptamine comparing the experimentally determined vibrational frequencies of six conformers to the results of *ab initio* calculations. The three torsional modes about the CC and CN bonds of the backbone allow to distinguish between the different conformers. As main reason for the different trends in vibrational frequencies for different conformers, we identified the different force constants due to the quite different interactions between the backbone and the chromophore. While the assignments of ground state vibrations on the basis of *ab initio* calculations is straightforward, excited state vibrations are harder to assign to a special mode, since the accuracy of theoretical methods for the excited states are generally smaller than for the ground state. Apart from comparison to the computed frequencies, intensity considerations based on the propensity rule guide the assignments of the excited state vibrations. Additionally, we could show that the vibronic corrections to the rotational constants in the electronically excited state contain sufficient information for an assignment of the torsional vibrations.

[1] J. R. Carney and T. S. Zwier, J. Phys. Chem. A **104**, 8677 (2000).
[2] L. A. Philips and D. H. Levy, J. Chem. Phys. **89**, 85 (1988).
[3] Y. R. Wu and D. H. Levy, J. Chem. Phys. **91**, 5278 (1989).
[4] T. Nguyen, T. Korter, and D. Pratt, Mol. Phys. **103**, 1603 (2005).
[5] M. Schmitt, M. Böhm, C. Ratzer, C. Vu, I. Kalkman, and W. L. Meerts, J. Am. Chem. Soc. **127**, 10356 (2005).
[6] M. Böhm and M. Schmitt (unpublished).
[7] L. L. Connell, T. C. Corcoran, P. W. Joireman, and P. M. Felker, Chem. Phys. Lett. **166**, 510 (1990).
[8] T. Nguyen and D. Pratt, J. Chem. Phys. **124**, 054317 (2006).
[9] W. Caminati, Phys. Chem. Chem. Phys. **6**, 2806 (2004).
[10] M. Schmitt, U. Henrichs, H. Müller, and K. Kleinermanns, J. Chem. Phys. **103**, 9918 (1995).
[11] W. Roth, C. Jacoby, A. Westphal, and M. Schmitt, J. Phys. Chem. A **102**, 3048 (1998).
[12] M. Schmitt, J. Küpper, D. Spangenberg, and A. Westphal, Chem. Phys. **254**, 349 (2000).
[13] S. Gerstenkorn and P. Luc, *Atlas du Spectre d'Absorption de la Molécule d'Iode* (CNRS, Paris, 1982).
[14] M. J. Frisch, G. W. Trucks, H. B. Schlegel *et al.*, GAUSSIAN 98, Revision a.11, Gaussian, Inc., Pittsburgh, PA, 2001.
[15] P. J. Stephens, F. J. Devlin, C. F. Chabalowski, and M. J. Frisch, J. Phys. Chem. **98**, 11623 (1994).
[16] C. Lee, W. Yang, and R. Parr, Phys. Rev. B **37**, 785 (1988).
[17] R. Ahlrichs, M. Bär, M. Häser, H. Horn, and C. Kölmel, Chem. Phys. Lett. **162**, 165 (1989).
[18] A. Schäfer, C. Huber, and R. Ahlrichs, J. Chem. Phys. **100**, 5829 (1994).
[19] F. Furche and R. Ahlrichs, J. Chem. Phys. **117**, 7433 (2003).

[20] R. Ahlrichs, M. Bär, H.-P. Baron, R. Bauernschmitt, S. Böcker, P. Deglmann, M. Ehrig, K. Eichkorn, S. Elliott, and F. Furche, TURBOMOLE, Version 5.6, Universität Karlsruhe, Germany, 2002.

[21] G. Varsanyi, *Assignments for Vibrational Spectra of 700 Benzene Deriva-tives* (Wiley, New York, 1974).

[22] M. Schmitt, R. Brause, C. Marian, S. Salzmann, and W. L. Meerts, J. Chem. Phys. (to be published).

[23] http://www-public.z.uni-duesseldorf.de/mschmitt/Gaussian_logs.html